AIAA 2003-4197

Thermal Contact Resistance of Non-Conforming Rough Surfaces, Part 1: Contact Mechanics Model

M. Bahrami, J. R. Culham, M. M. Yovanovich and G. E. Schneider
Microelectronics Heat Transfer Laboratory
Department of Mechanical Engineering
University of Waterloo, Waterloo
Ontario, Canada N2L 3G1

36th AIAA Thermophysics Conference
Meeting and Exhibit
June 23-26, 2003/Orlando, Florida

Thermal Contact Resistance of Non-Conforming Rough Surfaces, Part 1: Contact Mechanics Model

M. Bahrami*, J. R. Culham†, M. M. Yovanovich‡ and G. E. Schneider§
Microelectronics Heat Transfer Laboratory
Department of Mechanical Engineering
University of Waterloo, Waterloo
Ontario, Canada N2L 3G1

A new analytical model for spherical rough contacts, in the form of a set of relationships, is developed and solved numerically. It is shown that the maximum contact pressure is the parameter that specifies the contact pressure distribution. Simple correlations for calculating the maximum contact pressure and the radius of the macrocontact area as functions of the non-dimensional parameters are proposed. A relationship for pressure distributions is derived where the load is higher than the "critical" load. A general pressure distribution is developed which covers the entire range of spherical contacts from the smooth Hertzian to the conforming rough contact. Finally, a criterion is derived to identify flat surfaces where the surface curvature has negligible effect on the contact pressure.

NOMENCLATURE

A	=	area, (m^2)
a	=	radius of contact, (m)
a'_L	=	relative radius of macrocontact, a_L/a_{Hz}
a_s	=	radius of microcontacts, (m)
b	=	flux tube radius, (m)
c_0	=	function of τ, $1.8\ \tau^{-0.028}$
c'_0	=	function of τ, $0.31\ \tau^{0.056}$
c_1	=	Vickers microhardness coefficient, (GPa)
c_2	=	Vickers microhardness coefficient, $(-)$
d_v	=	Vickers indentation diagonal, (μm)
dr	=	increment in radial direction, (m)
E	=	Young's modulus, (GPa)
E'	=	equivalent elastic modulus, (GPa)
F	=	external force, (N)
F'	=	relative force error
f_i	=	discrete point forces, (N)
H_{mic}	=	microhardness, (GPa)
m	=	mean absolute surface slope, $(-)$
n_s	=	number of microcontacts
P	=	pressure, (Pa)
P'_0	=	relative maximum pressure, $P_0/P_{0,Hz}$
r, z	=	cylindrical coordinates
u	=	sphere profile, (m)
u_0	=	maximum indentation, (m)
Y	=	mean surface plane separation, (m)

Greek

α	=	non-dimensional parameter, $\sigma\rho/a^2_{Hz}$
β	=	summits radii of curvature, (m)
γ	=	general pressure distribution exponent
δ	=	max surface out-of-flatness, (m)
η_s	=	microcontacts density, $\left(m^{-2}\right)$
λ	=	dimensonless separation
ν	=	Poisson's ratio, $(-)$
ξ	=	dimensionless radial position, r/a_L
ρ	=	radius of curvature, (m)
σ	=	RMS surface roughness, (μm)
τ	=	non-dimensional parameter, ρ/a_{Hz}
ω_b	=	bulk normal deformation, (m)

Subscripts

0	=	value at origin
$1, 2$	=	surface 1, 2
a	=	apparent
b	=	bulk
c	=	critical
Hz	=	Hertz
L	=	large, macro
r	=	real
s	=	small, summit
v	=	Vickers

Introduction

An accurate knowledge of contact mechanics, i.e., pressure distribution, the size of contact area and the mean separation between surface planes as functions of applied load, geometrical and mechanical characteristics/properties of the contacting bodies, plays an important rule in predicting and analyzing thermal and electrical contact resistance and many tribological phenomena.

*Ph.D. Candidate, Department of Mechanical Engineering.
†Associate Professor, Director, Microelectronics Heat Transfer Laboratory.
‡Distinguished Professor Emeritus, Department of Mechanical Engineering. Fellow AIAA.
§Professor, Department of Mechanical Engineering. Associate Fellow AIAA.

The contact of two spherical rough surfaces includes two problems with different scales, i) the bulk or macro scale problem, i.e., bulk elastic compression which can be calculated using Hertz[1] theory for ideal *smooth* mean profiles of two surfaces, and ii) the small or micro scale problem, i.e., deformation of surface asperities. The scales of the sub-problems (macro and micro) are very different, yet at the same time, strongly interconnected. Due to surface roughness, contact between two surfaces occurs only at discrete microscopic contacts and the real area of contact, the total area of these microcontacts, is typically a small fraction of the nominal contact area.[2,3] The macrocontact area is defined as the area in which the microcontacts are distributed, also the contact pressure falls off to a negligible value at the edge of the macrocontact. The asperities act like a compliant layer on the surface of the contacting bodies, so that the contact is extended over a larger apparent area than it would be if the surfaces were smooth, and consequently, the contact pressure for a given load will be reduced.[4]

Developing an analytical model, which enables us to predict the contact parameters such as pressure distribution and the size of the macrocontact area, is the main goal of this study. It is also required to find simple correlations for determining the above contact parameters that can be used in analytical thermal contact models. Another purpose of this research is to find a criterion to define the *flat surface* where the surface curvature can be neglected.

Theoretical Background

As previously mentioned, the spherical rough contact mechanics problem is divided into macro and micro sub-problems. The macro problem is the contact of two spherical bodies, which in this study is assumed to be within the elastic limit, while the micro or the deformation of the surface asperities is assumed to be plastic.

Microcontact Modeling

The solution of any contact mechanics problem requires that the geometry of the intersection and overlap of the two undeformed surfaces be known as a function of their relative position. If the asperities of a surface are isotropic and randomly distributed over the surface the surface is called Gaussian. Williamson et al.[5] have shown experimentally that many of the techniques used to produce engineering surfaces give a Gaussian distribution of surface heights. Many researchers, including Greenwood and Williamson[3] assumed that the contact between two Gaussian rough surfaces can be simplified to the contact between a single Gaussian surface, having the effective (sum) surface characteristics, placed in contact with a perfectly smooth surface, as shown in Fig. 1. The equivalent

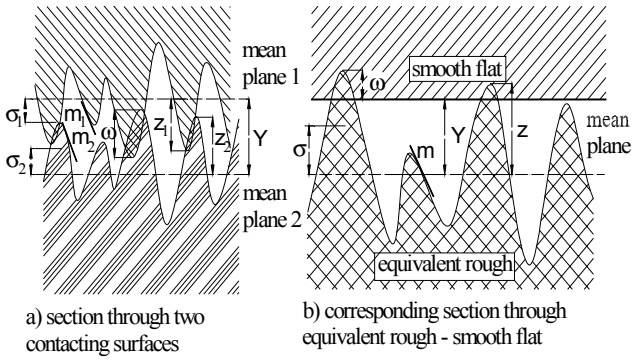

Fig. 1 Equivalent contact of conforming rough surfaces

roughness, σ, and surface slope, m, can be found from

$$\sigma = \sqrt{\sigma_1^2 + \sigma_2^2} \quad \text{and} \quad m = \sqrt{m_1^2 + m_2^2} \qquad (1)$$

Bahrami et al.,[6] based on the deformation mode of asperities, categorized existing microcontact mechanical models into three main groups: elastic, plastic, and elastoplastic. By comparing the elastic model of Greenwood and Williamson[3] and the plastic model of Cooper et al.[7] for nominal flat contacts, Bahrami et al.[6] showed that the behavior of the above models are similar, despite the different assumed deformation mode of asperities. They also concluded that in most real contacts, asperities deform plastically except for special cases where the surfaces are extremely smooth, see Bahrami et al.[6] for more detail.

The present model is developed assuming the asperities deform plastically. Plastic models assume that the asperities are flattened during contact. This is the same as assuming that the asperities penetrate into the smooth surface in the equivalent model, without any change in shape of the parts of the equivalent rough surface not yet in contact. Therefore, bringing two rough surfaces together within a distance, Y, is equivalent to removing the top of the asperities at a height Y above the mean plane. The assumption of pure plastic microcontacts enables the micro mechanics to be specified completely by the mean slope m and the surfaces roughness σ, without having to assume some deterministic peak shapes, as with elastic microcontact models. Cooper et al.[7] derived the following relationships for contact of nominal flat rough surfaces, assuming plastically deformed hemispherical asperities, whose height and surface slopes have Gaussian distributions, where the mean separation Y is constant throughout the con-

tact plane

$$\left.\begin{aligned} a_s &= \sqrt{\frac{8}{\pi}}\left(\frac{\sigma}{m}\right)\exp\left(\lambda^2\right)\operatorname{erfc}\,\lambda \\ n_s &= \frac{1}{16}\left(\frac{m}{\sigma}\right)^2\frac{\exp\left(-2\lambda^2\right)}{\operatorname{erfc}\,\lambda}A_a \\ \frac{A_r}{A_a} &= \frac{1}{2}\operatorname{erfc}\,\lambda \end{aligned}\right\} \qquad (2)$$

where $\lambda = Y/\sqrt{2}\sigma$, n_s, a_s, A_r and A_a are the dimensionless mean plane separation, number and average size of microcontacts, the real and the apparent contact area, respectively.

Microhardness

Microhardness is not constant throughout the material. Hegazy[8] demonstrated through experiments with four alloys that the effective microhardness is significantly greater than the bulk hardness. Microhardness decreases with increasing depth of the indenter until bulk hardness is obtained. He derived empirical correlations to account for the decrease in contact microhardness of the softer surface with increasing depth of penetration of asperities on the harder surface:

$$H_v = c_1\left(d'_v\right)^{c_2} \qquad (3)$$

where H_v is the Vickers microhardness in (GPa), $d'_v = d_v/d_0$ and $d_0 = 1\,(\mu m)$, d_v is the Vickers indentation diagonal in (μm), and c_1 and c_2 are correlation coefficients determined from the Vickers microhardness measurements.

Macrocontact Modeling

According to Johnson[4] in static frictionless contact of solids, the contact stresses depend only on the relative profile of the two surfaces, i.e., upon the shape of the interstitial gap before loading. Hertz[1] replaced the two spheres contact geometry by a flat surface and a profile, which results in the same undeformed gap between the surfaces. Additionally, all elastic deformations can be considered to occur in one body, which has an effective elastic modulus, E', and the other body is assumed to be rigid. The effective elastic modulus can be found from

$$\frac{1}{E'} = \frac{1-\upsilon_1^2}{E_1} + \frac{1-\upsilon_2^2}{E_2} \qquad (4)$$

where E and υ are the Young's modulus and Poisson's ratio, respectively. For the contact of two spheres, the effective radius of curvature is

$$\frac{1}{\rho} = \frac{1}{\rho_1} + \frac{1}{\rho_2} \qquad (5)$$

As a result of the above assumptions and by considering axisymmetric loading, the complex geometry of two spherical rough surfaces is simplified to a rigid smooth sphere having the equivalent radius of curvature in contact with a rough flat which has the equivalent surface characteristics, Fig. 2.

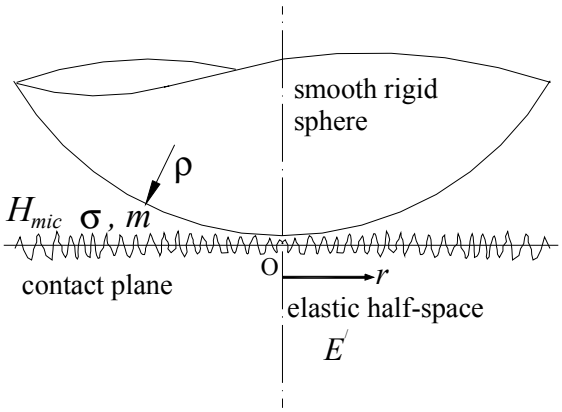

Fig. 2 Equivalent contact geometry of two spherical rough surfaces

The open literature contain very few analytical mechanical models for the contact of spherical rough surfaces. The first in-depth analytical study to investigate the effect of roughness on the pressure distribution and deformation of contacting elastic spherical bodies was performed by Greenwood and Tripp.[9] Greenwood and Tripp developed their model based on the same assumptions as the Greenwood and Williamson[3] nominal flat rough contact model. Their assumptions can be summarized as follows

- contact is axisymmetric and the bulk deformation is elastic
- rough surfaces are isotropic and have Gaussian height distribution with a standard deviation, σ
- the distribution of summit heights is the same as the surface heights standard deviation, i.e., $\sigma_s = \sigma$
- the deformation of each asperity is independent of its neighbors
- the asperity summits have a spherical shape all with a constant radius, β, the asperities entirely deform within the elastic limit and Hertz[1] theory can be applied for each individual summit.

They derived a geometrical relationship relating the local separation to the bulk deformation and the sphere profile. The elastic deformations produced by a pressure distribution over an area of the surface can be calculated by superposition, using the Boussinesq solution for a concentrated load on a half-space, and the fact that the displacement due to an axisymmetric pressure distribution will also be axisymmetric. It can be shown that the normal displacement in a half-space due to an arbitrary pressure distribution can be found

from[10]

$$\omega_b(r) = \begin{cases} \dfrac{2}{E'}\displaystyle\int_0^\infty P(s)\,ds & r = 0 \\ \dfrac{4}{\pi E' r}\displaystyle\int_0^r sP(s)\,K\left(\dfrac{s}{r}\right)ds & r > s \\ \dfrac{4}{\pi E'}\displaystyle\int_r^\infty P(s)\,K\left(\dfrac{r}{s}\right)ds & r < s \end{cases} \quad (6)$$

where $\omega_b(r)$ is the local bulk deformation, $K(\cdot)$ is the complete elliptic integral of the first kind, and s is a dummy variable. Greenwood and Tripp[9] used Eq. (6), which gave a complementary relation between local separation and the pressure. They reported a complete set of relationships and solved it numerically.

The most important trends in the Greenwood and Tripp[9] model were that an increase in roughness resulted in a decrease in the contact pressure, compared with the Hertzian pressure and the effective macroscopic contact radius grew beyond the Hertzian contact radius. The Greenwood and Tripp[9] model is attractive for its mathematical simplicity but it suffers from the following shortcomings:

- a constant summit radius β is unrealistic. For a random surface, β is also a random variable[11]
- two of its input parameters, i.e., radius of summits β and density of summits η_s cannot be measured directly and must be estimated through statistical calculations. These parameters are sensitive to the surface measurements[4]
- applying the model is complex and requires computer programming and numerically intensive solutions
- all asperities are assumed to deform elastically.

Tsukada and Anno[12] and Sasajima and Tsukada[13] with the same assumptions as Greenwood and Tripp[9] developed a model and offered expressions for pressure distribution as a function of non-dimensional maximum pressure, $P_0/P_{0,Hz}$, and non-dimensional radius of macrocontact area, a_L/a_{Hz}, for rough sphere-flat contacts. Tsukada and Anno[12] and Sasajima and Tsukada[13] presented these two parameters in a graphical form, in discrete curves, for relatively small radii of curvature, i.e., 5, 10, and 15 mm and roughness in the range of (0.1 to 2 μm). They did not report general expressions for the maximum pressure and the radius of macrocontact.

Present Model

The micro mechanical analysis of the present model is developed on the basis of the Cooper et al.[7] plastic model. The macrocontact area is divided into

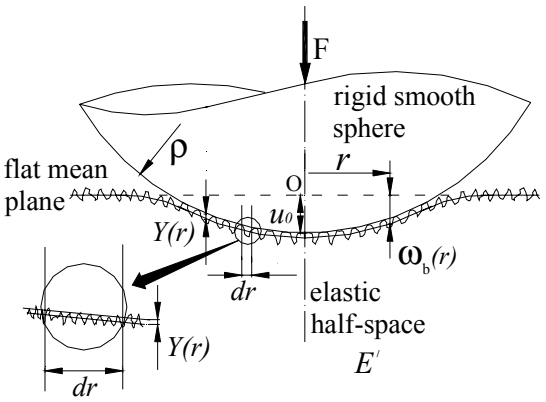

Fig. 3 Contact geometry after loading

infinitesimal conforming surface elements where the conforming rough surface relationships, i.e., Eqs. (2) can be applied. Bulk deformations are related to the local separation of the contacting surfaces, through a geometrical relationship similar to Greenwood and Tripp.[9] The assumptions of the present model can be summarized as:

- contacting surfaces are macroscopically spherical, which are considered as a sphere-flat contact, Fig. 2
- microscopically, contacting surfaces are rough and isotropic with a Gaussian asperity distribution. Only one surface is taken to be rough while the equivalent roughness is assumed to be on the flat plane and the sphere is assumed to be smooth
- microcontacts deform plastically and the asperity pressure is the local microhardness of the softer material in contact. Reasons supporting this assumption discussed in Bahrami et al.[6]
- deformation of each asperity is independent of its neighbors
- only the first loading cycle is considered
- the load is axisymmetric and the contact is frictionless, i.e., there are no tangential forces in the contact area
- the macrocontact is elastic where the elasticity theory given in Eq. (6) employed to determine the substrate deformation
- the contact is static, i.e., there is no relative motion or vibration effect.

In the vicinity of the contact region the profile of the sphere can be written as

$$u(r) = u_0 - r^2/2\rho \quad (7)$$

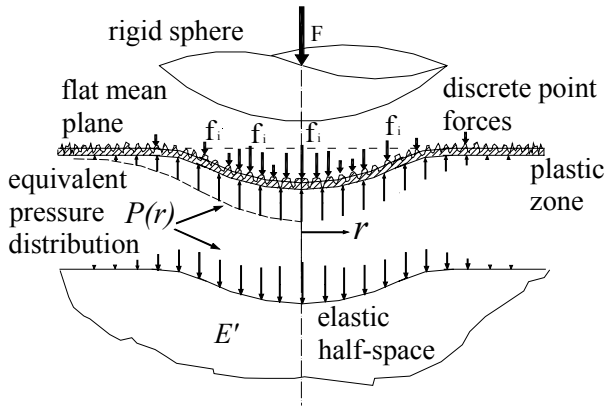

Fig. 4 Discrete point forces and the equivalent pressure distribution on the plastic zone

Figure 3 shows the contact geometry after applying the load. The local separation, $Y(r)$, is defined as the distance between two mean planes of the contacting surfaces and can be written as

$$Y(r) = \omega_b(r) - u(r) = \omega_b(r) - u_0 + r^2/2\rho \qquad (8)$$

At each microcontact a discrete point force is created as illustrated in Fig. 4. The sum of these discrete point forces must be equal to the external force, F. It is assumed that the asperities of the rough surface behave like a plastic zone on an elastic half-space, in the sense that the effect of the discrete point forces on the elastic half-space is considered as an equivalent continuous pressure distribution, $P(r)$. It should be noted that all bulk deformations are assumed to occur in the elastic half space which has an effective elasticity modulus E' and the sphere is assumed to be rigid. Consider an infinitesimal surface element, $dr \to 0$ where Fig. 3 shows a magnified element in which the local separation, $Y(r)$, is uniform. The ratio of real to apparent area for a surface element can be found from Eq. (2)

$$\frac{A_r(r)}{A_a(r)} = \frac{1}{2}\text{erfc}\,\lambda(r) \qquad (9)$$

where $A_a(r) = 2\pi r dr$. As a result of surface curvature, the mean local separation and consequently the mean size of the microcontacts vary with radial position. The local microhardness can be determined from the Vickers microhardness correlation, Eq. (3) as a function of the local mean microcontact radius. The relation between the Vickers diagonal d_v and the microcontact radius a_s, based on equal areas, is: $d_v = \sqrt{2\pi}a_s$. Therefore, the local microhardness is

$$H_{mic}(r) = c_1\left[\sqrt{2\pi}a_s(r)\right]^{c_2} \qquad (10)$$

where the local radius of the microcontacts can be found from Eq. (2)

$$a_s(r) = \sqrt{\frac{8}{\pi}}\left(\frac{\sigma}{m}\right)\exp\left[\lambda^2(r)\right]\ \text{erfc}\,\lambda(r) \qquad (11)$$

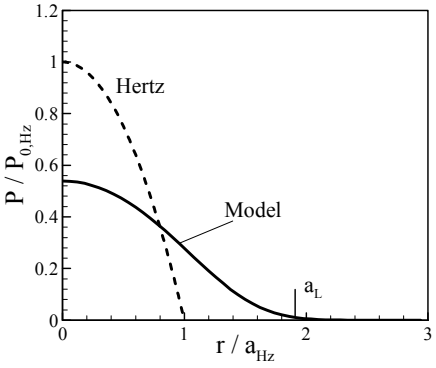

Fig. 5 Pressure distribution

The external load F is the summation of the point forces at the microcontacts

$$F = \sum_i \mathrm{f}_i = \iint\limits_{contact\ area} A_r(r)\, H_{mic}(r) \qquad (12)$$

Substituting Eq. (9) into Eq. (12)

$$F = \pi\int_0^\infty H_{mic}(r)\,\text{erfc}\,\lambda(r)\ \ rdr \qquad (13)$$

Instead of a_L, the upper limit of the integral is set to infinity, since the macrocontact radius is not known and the effective pressure distribution rapidly approaches zero. On the bulk side, the equivalent pressure must satisfy the force balance

$$F = 2\pi\int_0^\infty P(r)\, rdr \qquad (14)$$

The equivalent pressure distribution on the elastic half-space can be found from Eqs. (13) and (14)

$$P(r) = \frac{1}{2}H_{mic}(r)\,\text{erfc}\,\lambda(r) \qquad (15)$$

Knowing the pressure distribution, the normal displacement of the bulk can be found from Eq. (6). Eqs. (6), (8), (10), (11), (14), and (15) form a closed set of governing relationships. A computer program was developed to solve the set numerically. Appendix A describes the algorithm of the numerical solution.

No exact definition exists for the macrocontact radius in the literature. It is assumed in this study as the radius where the normalized pressure is negligible, i.e., $P(r = a_L)/P_0 < 0.01$.

Numerical Results

A simulation procedure was run to construct the results shown in Figs. 5 to 8, based on the algorithms described in Appendix A and by using input data shown in Table 1.

Figure 5 shows the pressure distribution predicted by the present model and the Hertzian pressure. It can

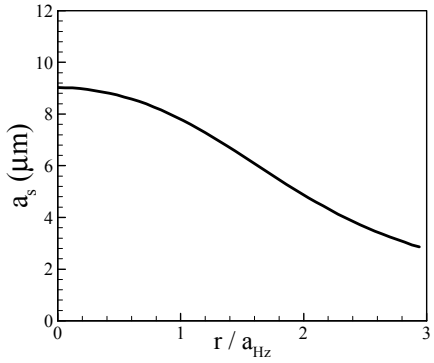

Fig. 6 Mean microcontacts radius

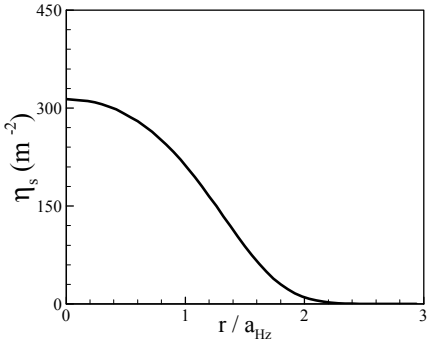

Fig. 7 Density of microcontacts

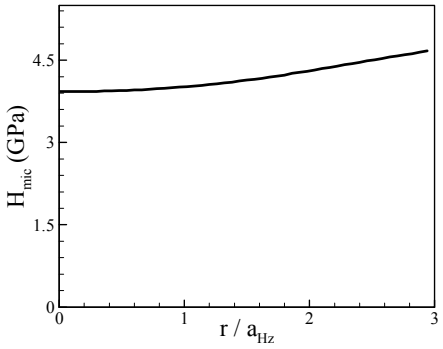

Fig. 8 Microhardness

Table 1 Input parameters for a typical contact

$\rho = 25\,(mm)$	$F = 50\,(N)$
$\sigma = 1.41\,(\mu m)$	$E' = 112.1\,(GPa)$
$m = 0.107\,(-)$	$c_1/c_2 = 6.27\,(GPa)\,/ -0.15\,(-)$

be seen that due to the presence of roughness the maximum contact pressure compared to the Hertzian, is reduced and the load is spread over a greater area. The predicted macrocontact radius a_L is also shown in Fig. 5. Unlike the Hertzian pressure, the effective pressure falls asymptotically to zero. As expected, the mean radius of microcontacts a_s, and microcontacts density η_s, decrease as the radial position r increases. The microhardness profile is shown in Fig. 8. To investigate

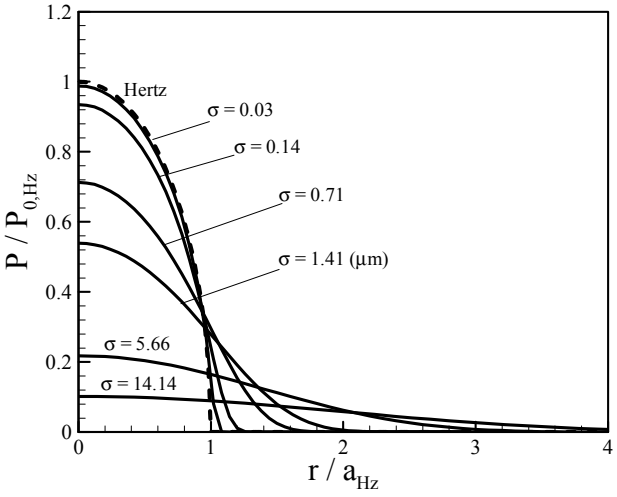

Fig. 9 Effect of roughness on equivalent pressure distribution

the effect of roughness on the pressure distribution, the program was run for a wide range of roughness from 0.02 to 14.4 (μm) while all other parameters in Table 1 were kept constant. Figure 9 illustrates the effect of roughness on the pressure distribution. It can be seen that the effective pressure distribution approaches the Hertzian pressure distribution as the roughness decreases.

Approximate Model

The main goal of this study is to develop simple correlations for determining the effective pressure distribution and the macrocontact radius as functions of non-dimensional parameters that describe the contact problem. To develop an approximate solution, the following simplifications are made:

- an effective microhardness H_{mic} which is constant throughout the contact region is considered
- the surface slope m is assumed to be a function of surface roughness, σ.

In this section, it is demonstrated that a general pressure distribution as a function of the maximum contact pressure exists. Then, using dimensional analysis the number of governing non-dimensional parameters is determined, and finally simple correlations for the maximum contact pressure and the macro contact radius are derived.

Figure 10 illustrates non-dimensional pressure distributions for some values of $P_0' = P_0/P_{0,Hz}$ as function of non-dimensional radial location $\xi = r/a_L$. It was observed that the non-dimensional pressure distribution can be specified as a function of the dimensionless maximum pressure P_0', and the radial position, ξ. In other words, a general profile exists that presents all possible pressure distributions.

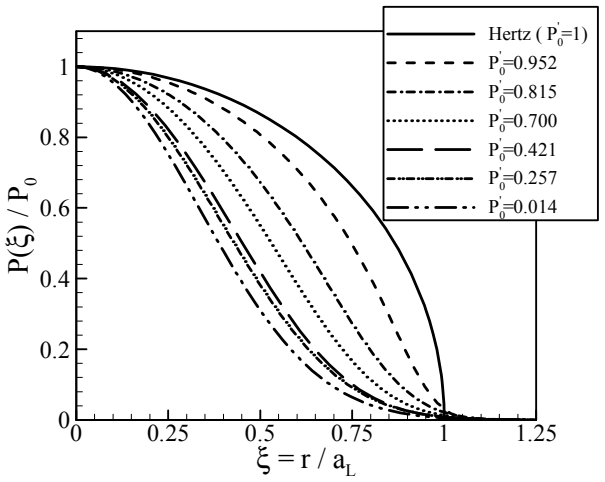

Fig. 10 Dimensionless pressure distributions for spherical rough surface contact

The Hertzian pressure distribution[1] where the contacting surfaces are perfectly smooth is:

$$P_{Hz}\left(r/a_{Hz}\right) = P_{0,Hz}\sqrt{1-\left(r/a_{Hz}\right)^2} \qquad (16)$$

where

$$P_{0,Hz} = \frac{3F}{2\pi a_{Hz}^2} \quad \text{and} \quad a_{Hz} = \left(\frac{3F\rho}{4E'}\right)^{1/3}$$

The profile of the pressure distribution, especially in the contacts where the dimensionless maximum pressure is less than 0.6, is very similar to a normal (Gaussian) distribution. However, as the dimensionless maximum pressure approaches one (the Hertzian contact) the pressure distribution begins to deviate from the normal distribution profile. The general profile for the pressure distribution for spherical rough surface contact was found to be

$$P\left(\xi\right) = P_0\left(1-\xi^2\right)^{\gamma} \qquad (17)$$

where $\xi = r/a_L$, and γ can be calculated through a force balance

$$F = 2\pi\int_0^{a_L} P\left(r\right) r dr \qquad (18)$$

Substituting Eq. (17) into (18), after evaluating the integral, one finds

$$\gamma = 1.5P_0'\ \left(a_L'\right)^2 - 1 \qquad (19)$$

where $P_0' = P_0/P_{0,Hz}$, and $a_L' = a_L/a_{Hz}$.

At the limit, where roughness approaches zero, P_0' and a_L' both approach one and $\gamma = 0.5$ and Eq. (17) yields the Hertzian pressure distribution, Eq. (16). Knowing the general pressure distribution profile, i.e., Eq. (17), the problem is reduced to find relationships for P_0 and a_L. Additionally, the radius of the macro-contact area, based on its definition, can be found if P_0 and the pressure distribution are known, therefore the key parameter is the maximum contact pressure, P_0.

Table 2 Physical input parameters and their dimensions for spherical rough contacts

Parameter	Dimension
Effective elastic modulus, E'	$ML^{-1}T^{-2}$
Force, F	MLT^{-2}
Microhardness, H_{mic}	$ML^{-1}T^{-2}$
Radius of curvature, ρ	M
Roughness, σ	M
Max. contact pressure, P_0	$ML^{-1}T^{-2}$

Dimensional Analysis

Dimensional analysis using the Buckingham Π theorem has been applied to many physical phenomena such as fluid flow, heat transfer and stress and strain problems. The Buckingham Π theorem proves that in a physical problem including n quantities in which there are m dimensions the quantities can be arranged into $n-m$ independent dimensionless parameters.[14] Table 2 summarizes the independent input parameters and their dimensions for spherical rough contacts. H_{mic} is an effective (mean) value for the microhardness of the softer material in contact.

The slope of the surface m may be estimated using an empirical relationship suggested by Lambert[15]

$$m = 0.076\ \sigma^{0.52} \qquad (20)$$

where σ is the surface RMS roughness in (μm).

The surface slope m is not considered as an independent input parameter since it can be determined from Eq. (20) as a function of surface roughness, therefore it is not included in Table 2.

All quantities in Table 2 are known to be essential to the maximum contact pressure and hence some functional relation must exist in the form of

$$P_0 = P_0\left(\rho, \sigma, E', F, H_{mic}\right) \qquad (21)$$

Applying the Buckingham Π theorem there will be three Π groups so the maximum pressure can be more compactly stated as a function of these three non-dimensional parameters. Johnson[4] following the Greenwood and Tripp[9] model, introduced a non-dimensional parameter α, that we may call the *roughness* parameter, as the ratio of roughness over the Hertzian maximum bulk deformation, $\omega_{0,Hz}$

$$\alpha = \frac{\sigma}{\omega_{0,Hz}} \equiv \frac{\sigma\rho}{a_{Hz}^2} = \sigma\left(\frac{16\rho E'^2}{9F^2}\right)^{1/3} \qquad (22)$$

The other non-dimensional parameters were chosen to be τ the *geometric* parameter, and E'/H_{mic} the *microhardness* parameter. The geometric parameter τ is defined as

$$\tau = \frac{\rho}{a_{Hz}} = \left(\frac{4E'\rho^2}{3F}\right)^{1/3} \qquad (23)$$

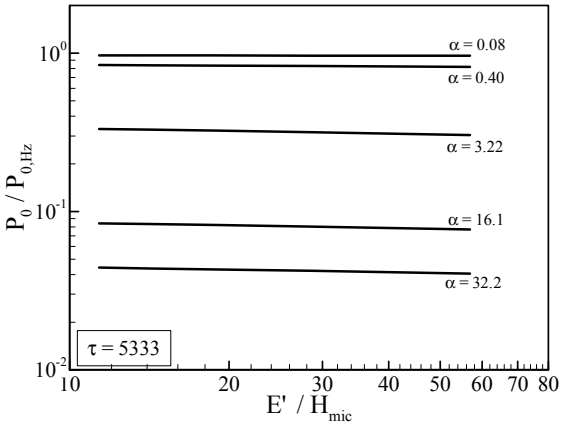

Fig. 11 Effect of microhardness on dimensionless maximum contact pressure

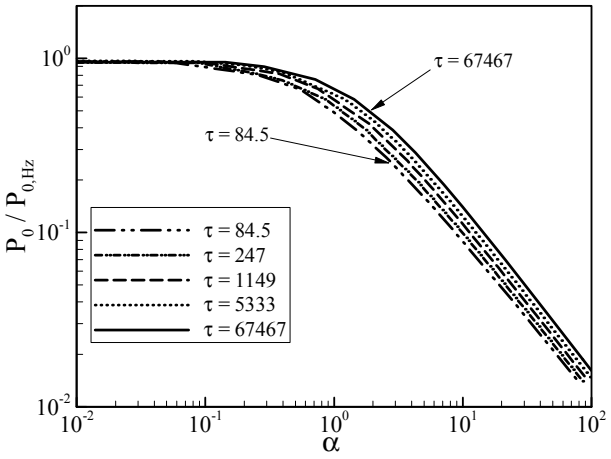

Fig. 12 Dimensionless maximum contact pressure

The computer program explained in the previous section was run for a wide range of input parameters to construct Figs. 11 - 13. As shown in Fig. 11, the effect of microhardness parameter E'/H_{mic}, on the maximum contact pressure was observed to be minimum and may be ignored. Figure 12 illustrates the dimensionless maximum contact pressure in the form of a family of curves for a wide range of α and τ. As α decreases, which is equivalent to a decrease in roughness or an increase in radius of curvature or load, the dimensionless maximum pressure approaches 1 (the Hertzian pressure). Figure 13 illustrates the macrocontact radius as a function of α and τ. As can be seen, by decreasing α, the dimensionless radius of contact approaches one (the Hertzian contact). Plots for the dimensionless maximum pressure and the macrocontact radius were curve fitted. The following expressions can be used to estimate the maximum dimensionless contact pressure and the dimensionless radius of contact, respectively

$$P_0' = \frac{P_0}{P_{0,Hz}} = \frac{1}{1 + 1.37\alpha\ \tau^{-0.075}} \qquad (24)$$

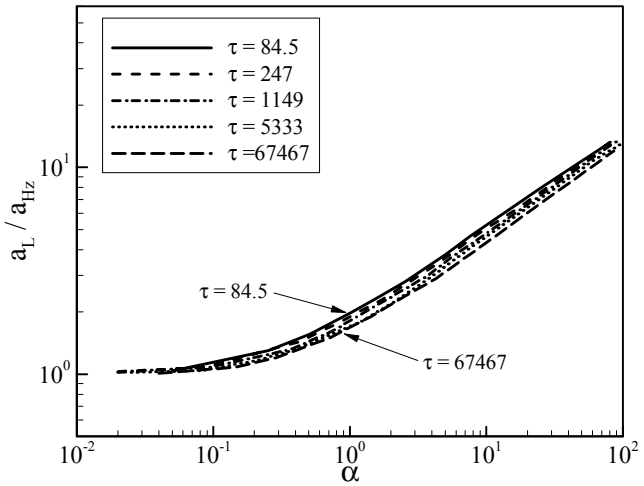

Fig. 13 Dimensionless radius of macrocontact

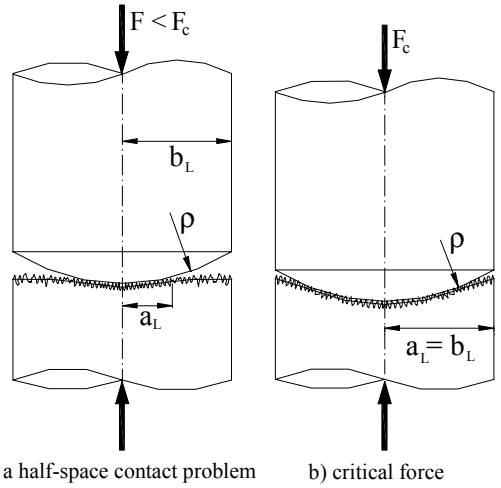

Fig. 14 Contact of two finite spherical rough bodies

$$a_L' = \frac{a_L}{a_{Hz}} = 1 - 1.50 \ln\ P_0' - 0.14 \ln^2\ P_0' - 0.11 \ln^3\ P_0' \qquad (25)$$

An expression for the non-dimensional radius of the macrocontact, a_L', was developed as a function of α and τ in the form of $a_L' = c_0\sqrt{\alpha + c_0'}$ where c_0 and c_0' are functions of τ only. In the limit where $\alpha \to 0$ (Hertzian contacts) as shown in Fig. 13, $a_L' \to 1$ therefore a relationship between c_0 and c_0' can be found such that $c_0' = (1/c_0)^2$. Thus, c_0 was curve-fitted and the following correlation for a_L' was obtained

$$a_L' = \frac{a_L}{a_{Hz}} = 1.80\frac{\sqrt{\alpha + 0.31\tau^{0.056}}}{\tau^{0.028}} \qquad (26)$$

The RMS difference between Eqs. (24) to (26) and the model is estimated to be less than 8 percent in the range of $0 \le \alpha \le 100$ and $50 \le \tau \le 80,000$.

Elastic Compression

In most engineering applications the size of the contacting bodies is finite and/or the radius of curvature is large, especially in the contacts where the surfaces are almost flat or slightly curved. When the above surfaces are placed in contact, by applying a specific force that we call the *critical force* the macrocontact area reaches to the boundaries of the contacting bodies, i.e., $a_L = b_L$, as shown in Fig. 14. By increasing the force beyond the critical force, the size of macrocontact remains constant but the contact pressure increases. Since the bulk deformation is assumed to be elastic, we refer to the above contact problems as *elastic compression*. Elastic compression cannot be treated as a half-space contact problem, since the half-space assumption cannot be justified especially in the regions close to the edge of the contacting bodies. The critical force, F_c, and the critical pressure distribution, the pressure distribution associated with the critical force for a specified spherical rough contact assembly are unique.

In contact stress theory the displacement at any point in the contact surface depends on the distribution of pressure throughout the whole contact. According to Johnson[4] the above interconnection may be avoided if the solids are modeled by a simple Winkler elastic foundation rather than a half-space. As illustrated in Fig. 15, the elastic compression approximation implies that as load passes the critical load the elastic foundation, which rests on a rigid base, is compressed by the rigid spherical indenter. There is no interaction between the springs of the model, i.e., shear between adjacent elements of the foundation is ignored. Therefore, contact pressure at any point depends only on the displacement at that point. Equation (17) can be used to calculate the contact pressure distribution, where the external force is less than or equal to the critical load. Beyond the critical load where $F > F_c$, the size of the macrocontact remains constant and the elastic foundation approximation is used to determine the pressure distribution. Assuming the elastic foundation approximation, a uniform increase will be added to the critical pressure distribution at each point in the contact area. Therefore, the general pressure distribution can be summarized as

$$P(\xi) = \begin{cases} P_0 \left[1-\xi^2\right]^{\gamma} & F \le F_c \\ P_{0,c} \left[1-\xi^2\right]^{\gamma_c} + \dfrac{F-F_c}{\pi b_L^2} & F \ge F_c \end{cases} \tag{27}$$

where $a_L = b_L$ for $F \ge F_c$, $P_{0,c}$, and γ_c are the maximum pressure and the exponent of the critical pressure distribution, respectively. Figure 16 shows the predicted pressure distributions for some values of the external load as an example. The parameters of the contact are: $\rho = 10\,(m)$, $E' = 112\,(GPa)$, $\sigma = 2\,(\mu m)$, and $b_L = 12\,(mm)$.

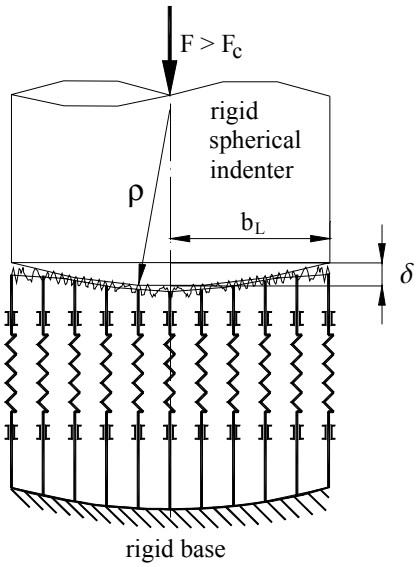

Fig. 15 Elastic foundation, Winkler model

To find a relationship for the critical force, Eqs. (24) and (25) should be solved simultaneously where $a_L = b_L$, which leads to an implicit relation, and requires an iterative solution. To avoid the iterative solution, the following approximate expression for a_L is offered

$$a'_L = 1.5\sqrt{\alpha + 0.45} \tag{28}$$

The above correlation is only a function of α, and it was developed for contacts where the effective radius of curvature is relatively large, i.e., the situations where the elastic compression more likely occurs. Using Eq. (28), the critical force can be estimated from

$$F_c = \frac{4E'}{3\rho}\left[\max\left\{0, \left(b_L^2 - 2.25\sigma\rho\right)\right\}\right]^{3/2} \tag{29}$$

where $\max\{x, y\}$ returns the maximum value between x and y.

A criterion for defining the flat surface, where the surface curvature has negligible effect on the pressure distribution can be derived by setting $F_c = 0$. Setting F_c equal to zero means that with applying no load $a_L = b_L$, thus the contacting surfaces are practically flat, which leads to

$$\frac{b_L^2}{\sigma\rho} \le 2.25 \tag{30}$$

For spherical surfaces, Clausing and Chao[16] used a geometrical expression that relates the maximum out-of-flatness, δ (see Fig. 15) to the radius of curvature

$$\rho = \frac{b_L^2}{2\delta} \tag{31}$$

Combining Eqs. (30) and (31), the flat surface criterion in terms of surface out-of-flatness can be obtained

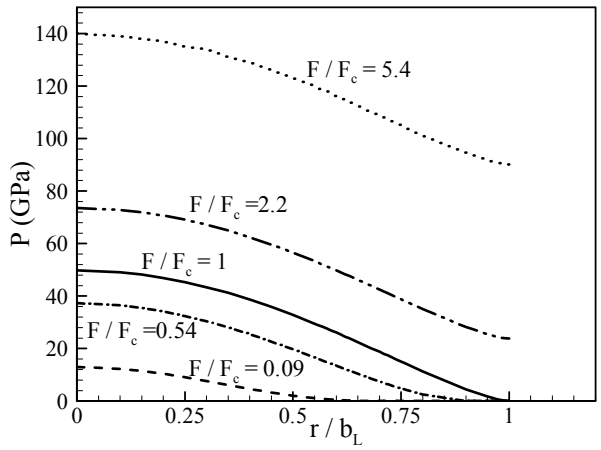

Fig. 16 Contact pressure distribution

as

$$\frac{\delta}{\sigma} \leq 1.12 \tag{32}$$

In other words, if the out-of-flatness and the roughness of a surface are in the same order of magnitude, the surface is flat.

Concluding Remarks

The mechanical contact of spherical rough surfaces was studied and a new analytical model was developed. The deformations of surface asperities were considered to be plastic while the bulk deformation was assumed to remain within the elastic limit.

A closed set of governing relationships was derived and solved numerically. A computer code was developed to solve the governing relationships. The algorithm of the numerical procedure is explained in Appendix A. The pressure distributions predicted by the model were plotted for different values of surface roughness and it was seen that as the surface roughness approaches zero the predicted pressure distribution approaches the Hertzian pressure.

Additionally, it was shown that a general pressure distribution profile exists that encompasses all spherical rough contacts. The maximum contact pressure was observed to be the key parameter that specifies the contact pressure distribution. The suggested general pressure distribution expression yields the Hertzian contact pressure at the limit, where roughness is set to zero.

Using dimensional analysis, the number of independent non-dimensional parameters that describe the maximum contact pressure was determined to be three, the roughness α, the geometric τ, and the microhardness E'/H_{mic} parameters. The effect of the microhardness parameter E'/H_{mic} on the maximum contact pressure was observed to be small and ignored. Using curve-fitting techniques, simple correlations were suggested for calculating the maximum contact pressure distribution and the radius of the macrocontact area, as functions of roughness α, and geometric parameters τ.

An expression for estimating the critical load was derived, where $a_L = b_L$. The Winkler approximation was used to derive a relationship for the contact pressure distributions, where the loads are higher than the critical load. This expression along with the above correlation formed a general pressure distribution that encompasses the possible contact cases ranging from the smooth Hertzian to the conforming rough contact.

Also a criterion was offered to identify the flat surface, where the effect of surface curvature on the contact pressure can be neglected. Based on this criterion, the surface can be considered flat if the surface out-of-flatness and roughness are in the same order of magnitude.

The advantages of the present model over the Greenwood and Tripp[9] (GT) model are:

- the present model requires two input surface parameters, roughness σ, and surface slope m. The GT model needs three input parameters, i.e., σ, β, and η
- unlike the summit radius β and the microcontact density η in the GT model, the present model input parameters can be measured directly and they are not sensitive to the surface measurements
- a pressure distribution profile was proposed as a function of the maximum contact pressure which covers all possible contact cases
- simple correlations for determining the maximum contact pressure and the radius of macrocontact as functions of two non-dimensional parameters, i.e., the roughness parameter α and the geometric parameter τ were offered.

References

[1]Hertz, H., "On the Contact of Elastic Bodies," *Journal fur die reine und angewandie Mathematic, (in German)*, Vol. 92, 1881, pp. 156–171.

[2]Tabor, D., *The Hardness of Metals*, Oxford University Press, Amen House, London E.C.4, UK, 1951.

[3]Greenwood, J. A. and Williamson, B. P., "Contact of Nominally Flat Surfaces," *Proc., Roy. Soc., London, A295*, 1966, pp. 300–319.

[4]Johnson, K. L., *Contact Mechanics*, Cambridge University Press, Cambridge, UK., 1985.

[5]Williamson, J. B., Pullen, J., Hunt, R. T., and Leonard, D., "The Shape of Solid Surfaces," *Surface Mechanics, ASME, New York*, 1969, pp. 24–35.

[6]Bahrami, M., Culham, J. R., Yovanovich, M. M., and Schneider, G. E., "Review Of Thermal Joint Resistance Models For Non-Conforming Rough Surfaces In A Vacuum," *Paper No. HT2003-47051, ASME Heat Transfer Conference, July 21-23, Rio Hotel, Las Vegas, Nevada*, 2003.

[7]Cooper, M. G., Mikic, B. B., and Yovanovich, M. M., "Thermal Contact Conductance," *International Journal of Heat and Mass Transfer*, Vol. 12, 1969, pp. 279–300.

[8]Hegazy, A. A., *Thermal Joint Conductance of Conforming Rough Surfaces: Effect of Surface Micro-Hardness Variation*, Ph.D. thesis, University of Waterloo, Dept. of Mech. Eng., Waterloo, Canada, 1985.

[9]Greenwood, J. A. and Tripp, J. H., "The Elastic Contact of Rough Spheres," *Transactions of the ASME: Journal of Applied Mechanics*, Vol. 89, No. 1, 1967, pp. 153–159.

[10]Gladwell, G. M. L., *Contact Problems in the Classical Theory of Elasticity*, Alphen aan den Rijn: Sijthoff and Noordhoff, The Netherlands, Germantown, Maryland, USA, 1980.

[11]Francis, H. A., "Application of Spherical Indentation Mechanics To Reversible and Irreversible Contact Between Rough Surfaces," *Wear*, Vol. 45, 1976, pp. 221–269.

[12]Tsukada, T. and Anno, Y., "On the Approach Between a Sphere and a Rough Surface (1st. Report- Analysis of Contact Radius and Interface Pressure," *Journal of the Japanese Society of Precision Engineering (in Japanese)*, Vol. 45, No. 4, 1979, pp. 473–479.

[13]Sasajima, K. and Tsukada, T., "On the Approach Between a Sphere and a Rough Surface (2nd. Report- Critical Condition to Yield Plastic Deformation in Contacting Bodies," *Journal of the Japanese Society of Precision Engineering (in Japanese)*, Vol. 47, No. 6, 1981, pp. 694–699.

[14]Streeter, V. L. and Wylie, E. B., *Fluid Mechanics*, McGraw-Hill Book Company, New York, 1975.

[15]Lambert, M. A., *Thermal Contact Conductance of Spherical Rough Metals*, Ph.D. thesis, Texas A & M University, Dept. of Mech. Eng.,Texas, USA, 1995.

[16]Clausing, A. M. and Chao, B. T., "Thermal Contact Resistance in a Vacuum Environment," *Paper No.64-HT-16, Transactions of ASME: Journal of Heat Transfer*, Vol. 87, 1965, pp. 243–251.

Appendix A: Numerical Procedure

The following procedure, Fig. 18, is used to solve the governing set of relationships outlined in the present model. A value of $u_{0,1}$ is assumed, pressure distribution can be computed. $P(r)$ is then used to calculate an improved $\omega_b(r)$. This improved $\omega_b(r)$ now is used to calculate a new pressure distribution $P_{new}(r)$, and so on until $P(r)$ converges. The algorithm of the above procedure is shown in the inner loop flow chart, Fig. 17. The pressure distribution $P(r)$ is integrated and compared with the external load F and the relative force error F_1^* is calculated. $u_{0,2}$ is assumed and all the above-mentioned steps are repeated for $u_{0,2}$ to compute F_2^*. Using linear interpolation; u_{new} and then F_{new}^* are similarly calculated by using the inner loop procedure. If F_{new}^* is not within the acceptable tolerance, u_0 and F^* are updated and the iterative pressure-displacement calculation procedure is repeated until the convergence is achieved. The loop is continued until the integrated pressure and external load are within an acceptable tolerance.

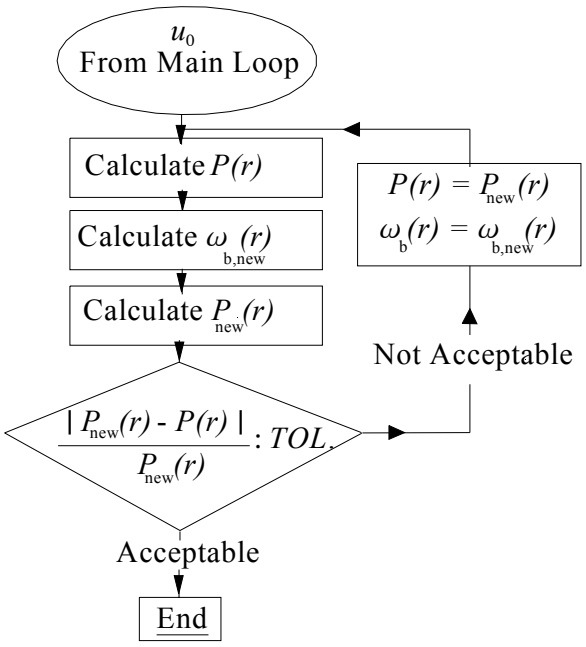

Fig. 17 Pressure-displacement iteration procedure, the inner loop

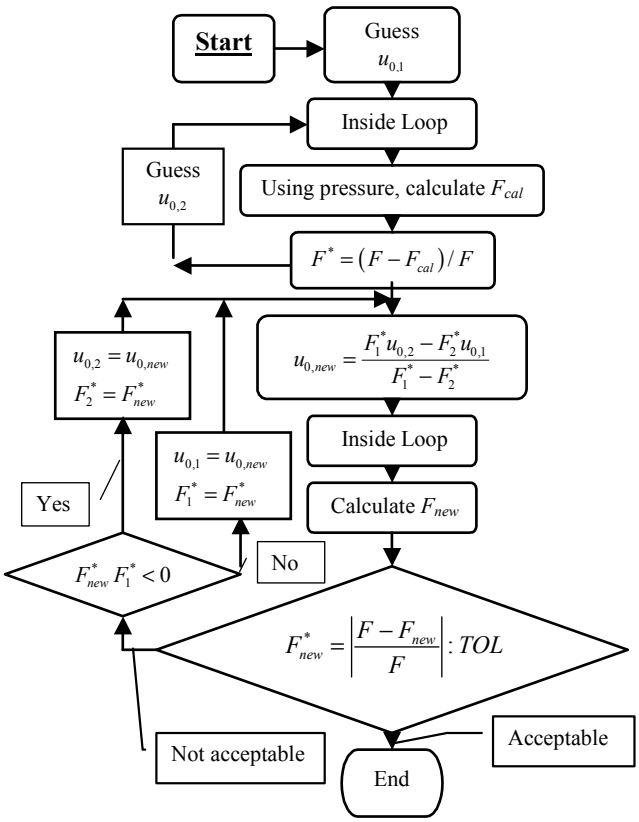

Fig. 18 Numerical algorithm